NOTE *Internal Medicine*

Computed tomographic images of discospondylitis in a calf

Takeshi TSUKA[1)]*, Naoki YAMAMOTO[2)], Makoto SANESHIGE[2)], Takehito MORITA[1)], Yuji SUNDEN[1)], Yusuke MURAHATA[1)], Kazuo AZUMA[1)], Tomohiro OSAKI[1)], Norihito ITO[1)], Yoshiharu OKAMOTO[1)] and Tomohiro IMAGAWA[1)]

[1)]*Department of Veterinary Clinical Medicine, School of Veterinary Medicine, Tottori University, 4–101 Koyama-Minami, Tottori 680–8553, Japan*
[2)]*Shimane Prefectural Federation Agricultural Mutual Aid Association, 105 Tonomachi, Matsue, Shimane 690–0887, Japan*

(Received 1 April 2015/Accepted 9 July 2015/Published online in J-STAGE 8 August 2015)

ABSTRACT. A 2-month-old male Japanese Black calf was presented with a 30-day history of progressive ataxia. Antemortem examination using computed tomography (CT) revealed narrowing of the disc spaces due to destruction of intervertebral structures between the first and second thoracic vertebrae and between the second and third thoracic vertebrae. Osteolysis was evident as irregular hypoattenuating lesions within the opposing end plates of the first, second and third thoracic vertebrae. Pseudomonas aeruginosa was detected as the causative bacteria, and discospondylitis was diagnosed. To the best of our knowledge, this is the first bovine case report describing the application of CT for the diagnosis of discospondylitis.

KEY WORDS: calf, computed tomography, discospondylitis, *Pseudomonas aeruginosa*, radiography

doi: 10.1292/jvms.15-0194; *J. Vet. Med. Sci.* 77(12): 1689–1691, 2015

Discospondylitis is an infection of the intervertebral disc (as discitis) and adjacent vertebral bodies (as osteomyelitis or spondylitis) [10]. Radiography is a common diagnostic tool for identifying discospondylitis in animals [10]. The earliest radiographic signs are irregularity of the vertebral end plates and narrowing of the disc spaces due to destruction of the disc structures [10]. During the progressive process, lytic lesions are modified by the formation of sclerosis and bridging within the intervertebral spaces, followed by complete fusion of the two affected vertebrae [6]. However, errors in diagnosis of discospondylitis sometimes occur, because the earliest radiographic signs are too subtle [5]. Computed tomography (CT) allows a presumptive diagnosis of discospondylitis in small animal practice, because it can visualize the earliest signs including slight osteolytic changes [5].

A 2-month-old male Japanese Black calf with a body weight of 55 kg presented with a 30-day history of progressive ataxia. Clinical signs did not respond to treatment with selenium, vitamin E, vitamin B1 or antibiotics (oxytetracycline 2 times and orbifloxacin 8 times). On admission, the calf showed stiff gait and an abnormal standing posture with the forelimbs and hindlimbs positioned under the body with arching of the back. Neurological examination revealed a lack of proprioception and placing reaction and a weakened withdrawal reflex in the left forelimb. Postural reflexes were also weak in the right forelimb. No neurological deficit was observed in the hindlimbs, although the calf showed staggered walking in the hindlimbs. The white blood cell count (18,700/*µl*), aspartate amino transferase level (265 U/*l*) and creatine phosphokinase level (806 U/*l*) were all elevated.

Imaging examinations were performed under general anesthesia with 0.2–0.3% isoflurane after sedation with 0.3 mg/kg xylazine hydrochloride. Radiographic examination using computed radiography (REGIUS Console CS-3, Konica Minolta Healthcare Co., Ltd., Tokyo, Japan) revealed narrowing of the intervertebral spaces between the first thoracic (T1) and T2 vertebrae than that between C7 and T1 (Fig. 1). The intervertebral space between T2 and T3 was wider than that between T3 and T4 due to the osteolytic changes in the caudal edge of the T2 end plate and the cranial edge of the T3 end plate. Lysis was evident in the caudal part of the end plate of T1, adjacent to the intervertebral space between T1 and T2. The length of the vertebral body of T2 was shorter in the cranial-caudal direction than in the normal vertebra. Bony proliferation and bridging were not evident in the vertebral bodies of T1 to T3. CT examination using a 16-row multidetector helical scanner (ECLOS, Hitachi Medical Co., Ltd., Tokyo, Japan) revealed an oval-shaped focal lesion at the center of the caudal T1 end plate in transverse CT images (Fig. 2A). The lesion was hypoattenuating compared with the surrounding vertebral body. On the transverse CT showing the ventral body of T2, a hypoattenuating lesion had destroyed the ventral edge of the cranial part of the end plate (Fig. 2B). Bony margins were well-defined and smooth on the caudal edge of the C7 end plate and the cranial edge of the T1 end plate. At the T1–T2 intervertebral space, the hypoattenuated area spread into the T1 vertebral body. This extension caused an irregular, deeply concave lesion in the T1 end plate. The cranial and caudal T2 end plates were also irregular. The length of the T2 vertebral body was shorter than those of the other vertebra. Very mild bony proliferation

*CORRESPONDENCE TO: TSUKA, T., Department of Veterinary Clinical Medicine, School of Veterinary Medicine, Tottori University, 4–101 Koyama-Minami, Tottori 680–8553, Japan.
e-mail: tsuka@muses.tottori-u.ac.jp

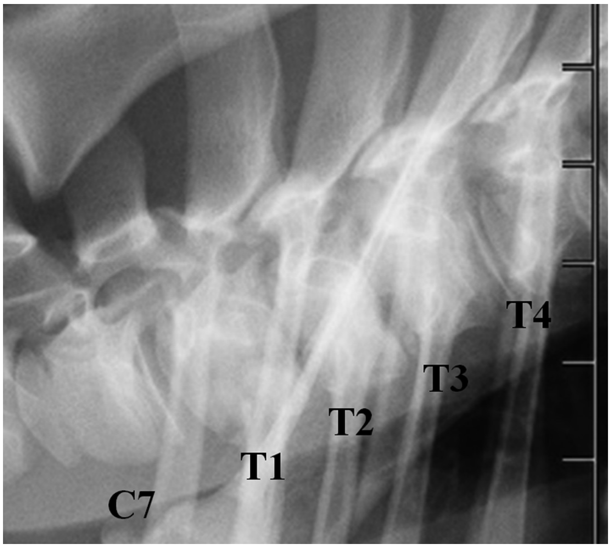

Fig. 1. Lateral radiograph of the cervical-thoracic vertebrae. Osteolysis is evident in the caudal part of the end plate of the first thoracic vertebra. Osteolytic changes cause reduced length of the second thoracic vertebra. Bar=25 mm.

was present in the T1–T2 and T2–T3 intervertebral spaces.

The calf was euthanized at the request of the owner based on the poor prognosis for complete recovery.

Gross examination revealed that the structures of the end plates were irregular due to osteolytic destruction at the caudal edge of T1 and the cranial and caudal edges of T2 (Fig. 3B). The vertebral body of T2 was shortened due to osteolysis from both sides. A deep concave lytic space present at the caudal T1 vertebral body was filled with dark-red necrotic material. No visible abnormalities were evident in the spinal cord. No lesions were apparent within the body cavity. Histopathologically, proliferation of granulation tissues characterized by infiltration of neutrophils, macrophages and lymphocytes was observed within the caudal T1 end plate and cranial T2 end plate (Fig. 4). The spinal cord close to the T1–T2 region showed no significant pathological changes. *Pseudomonas aeruginosa* was cultured from a swab obtained from the T1–T2 intervertebral space.

The most common cause of discospondylitis is hematogenous spread of a bacterial or fungal infection from a primary infective focus [4, 6, 7]. In the present case, the primary lesion was not discovered for hematogenous spread of *P. aeruginosa* infection to the T1 to T3 intervertebral spaces. Causative microbes and primary lesions are frequently undetermined in affected animals [2].

The radiographic image in the present case depicted abnormal disc spaces with poorly defined end plates and reduced length of the vertebral body. It contained enough diagnostic information for us to suspect osteomyelitis or discospondylitis within T1 to T3 in the present case. These radiographic abnormalities may be identical to the early radiographic signs, which predict destruction of the disc structures and osteomyelitis (totally discospondylitis) occurring in T1 to T3

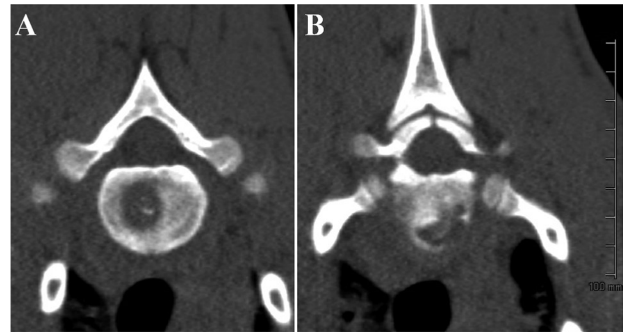

Fig. 2. Transverse computed tomography of the thoracic vertebra. (A) An oval-shaped focal lesion is evident at the center of the caudal part of the end plate of the first thoracic vertebra. (B) The hypoattenuating lesion has destroyed the ventral edge of the cranial part of the end plate of the second thoracic vertebra. No bony proliferation is apparent in the first or second thoracic vertebrae. Bar=10 mm.

[10]. However, the earliest signs are not always indicative of the occurrence of discospondylitis because of a lack of or only slight visualization of the earliest osteolytic lesions [5]. The most commonly affected regions of discospondylitis are the caudal cervical and cranial thoracic vertebral columns in cattle as in the present case [2, 4, 7, 11]. Great differences have been reported among species in the common affected regions of discospondylitis: the thoracolumbar vertebral column (the L7–S1 intervertebral space in particular) in dogs [10], lumbosacral vertebral column in pigs [3] and C3–C4 intervertebral space in a llama with Pseudomonas-associated discospondylitis [8]. The horse may not have the common affected regions, because the lesions were located on C3–C4 or L3–L4 intervertebral spaces in two previous cases [9]. Occurrence in the caudal cervical and cranial thoracic vertebral columns may allow less prominent bony lesions to be missed in radiographic images, because subtle radiographic abnormalities may be completely obscured by radiographic shadows of the thick muscular layers and the shoulder structure compared with the occurrence in thoracolumbar or lumbosacral vertebral columns. Diagnosis of discospondylitis may be advanced by use of myelography for observation of spinal cord compression, which is the most common cause of neurological deficits caused by the proliferation of inflammatory tissue and exostosis. Moreover, cerebrospinal fluid, which is collected in the process of myelography, may be useful for observations of the degeneration, increase in inflammatory cell count and detection of pathogenic microorganisms [11].

A tentative diagnosis can be confirmed on CT [7]. CT can visualize destruction of the end plate and osteolysis, which are the common bony lesions in discospondylitis, as areas of hypoattenuation [1]. Hypoattenuating signs are easily discriminated, because of the relatively good contrast with adjacent hyperattenuating bony structures [1]. CT may visualize majority of osteolytic changes at any stage of discospondylitis, although advances in bony proliferative changes related to progressive stages may make it difficult to identify

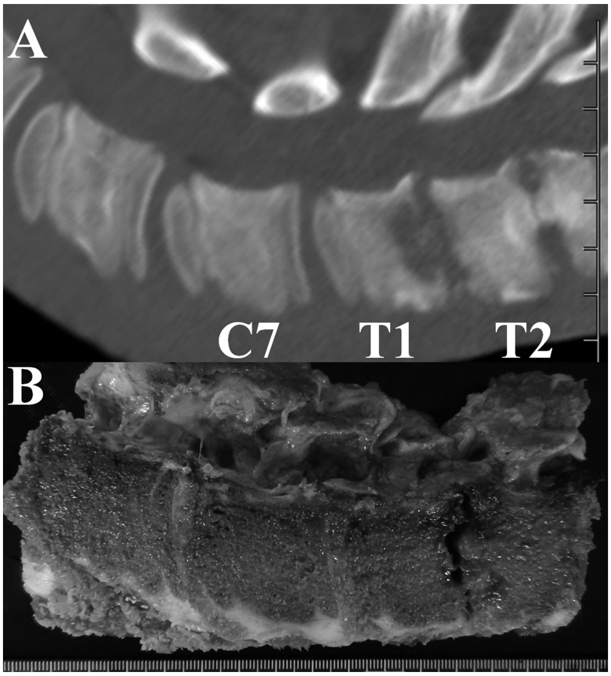

Fig. 3. Sagittal reconstructed computed tomography (A) and gross appearance (B) of the cervical-thoracic vertebrae. A deeply concave osteolytic lesion, showing hypoattenuation on CT, is filled with dark-red necrotic material within the caudal part of the end plate of the first thoracic vertebra. Osteolysis is grossly evident within the cranial and caudal parts of the end plate of the second thoracic vertebra, which appears as a shortened vertebral body with irregular edges at either end on CT. Bar=10 mm.

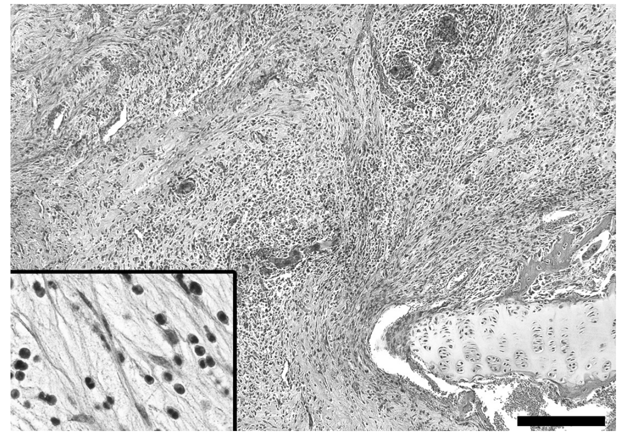

Fig. 4. Histopathology of the cranial end plate of the second thoracic vertebral bone. The bony architecture is replaced by severe inflammatory cells. These cells mainly consist of neutrophils and spindle-shaped fibroblastic cells (inset). The remaining cartilaginous tissue of the vertebra is located at the lower right. Bar=200 μm.

such lesions on radiographic images [1, 2, 5]. Another useful function of CT is the reconstruction of two-dimensional (2D) sections from every view. Transverse CT images, which are a basic section primarily obtained during CT scanning, enable evaluation of left-right symmetry of the vertebral structure and the spinal cord. The majority of these lesions compressing the spinal cord tend to show dominance of one side or the other [4]. Sagittal reconstructed 2D images can visualize the positional relationships between multiple vertebra and intervertebral disc structures. Such images allow a simple longitudinal view to observe the running of the spinal cord and positioning of multiple lesions, as sometimes seen in previous cases [5, 11]. Causes of mechanical compression of the spinal cord due to discospondylitis include displacement of vertebrae due to instability, distortion of the intervertebral foramen, protrusion of infected disc material and bony proliferations between affected vertebrae [2, 4]. Unfortunately, CT is less advantageous for visualizing the pathological changes of inflammation, necrosis and deformation within the spinal cord. However, such lesions may be identified by use of myelography in CT examinations. The diagnosis of discospondylitis in bovine practice may be facilitated by evaluating more affected animals with radiographs and CT in order to develop a classification of the bony changes corresponding to the various stages of infection. This may allow diagnosis of the earliest stage of discospondylitis and subsequently successful treatment.

REFERENCES

1. Betbeze, C. and McLaughlin, R. 2002. Canine diskospondylitis: Its etiology, diagnosis, and treatment. *Vet. Med.* **97**: 673–681.
2. Braun, U., Flückiger, M., Gerspach, C. and Grest, P. 2003. Clinical and radiographic findings in six cattle with cervical diskospondylitis. *Vet. Rec.* **152**: 630–632. [Medline] [CrossRef]
3. Doige, C. E. 1980. Discospondylitis in swine. *Can. J. Comp. Med.* **44**: 121–128. [Medline]
4. Hammond, G., Van Winden, W. and Philbey, A. 2006. Diskospondylitis and umbilical abscessation in a calf. *Vet. Rec.* **158**: 600–601. [Medline] [CrossRef]
5. Moore, M. P. 1992. Discospondylitis. *Vet. Clin. North Am. Small Anim. Pract.* **22**: 1027–1034. [Medline] [CrossRef]
6. Muggli, E., Schmid, T., Hagen, R., Schmid, B. and Nuss, K. 2011. Diagnosis and treatment of lumbosacral discospondylitis in a calf. *BMC Vet. Res.* **7**: 53. [Medline] [CrossRef]
7. Paiva Della Libera, A. M., Leal, M. L., Gregory, L., Rodrigues da Silva, D. Y., Unruh, S. M., Birgel Júnior, E. H. and Benesi, F. J. 2004. Cervical diskospondylitis in a calf: clinical, radiographic, and necroscopy findings. *Can. Vet. J.* **45**: 700–701. [Medline]
8. Sura, R., Creden, A. and Van Kruiningen, H. J. 2008. Pseudomonas-associated discospondylitis in a two-month-old llama. *J. Vet. Diagn. Invest.* **20**: 349–352. [Medline] [CrossRef]
9. Sweers, L. and Carstens, A. 2006. Imaging features of discospondylitis in two horses. *Vet. Radiol. Ultrasound* **47**: 159–164. [Medline] [CrossRef]
10. Thomas, W. B. 2000. Diskospondylitis and other vertebral infections. *Vet. Clin. North Am. Small Anim. Pract.* **30**: 169–182, vii. [Medline] [CrossRef]
11. Zani, D. D., Romanò, L., Scandella, M., Rondena, M., Riccaboni, P., Morandi, N., Lombardo, R., Di Giancamillo, M., Belloli, A. G. and Pravettoni, D. 2008. Spinal epidural abscess in two calves. *Vet. Surg.* **37**: 801–808. [Medline] [CrossRef]